# Lecture 20. Coherent structures in turbulence

Outline

- Stochastic/statistical v.s. structural/dynamical views of turbulence
- Large-scale coherent structures
- Geometry of small-scale turbulence
- Data-driven coherent structure eduction

# 0. Motivations, stochastic v.s. structural views of turbulence

**Statistical/stochastic view:**

correlation functions, spectra, ‘structure’ functions, probability density functions (PDFs), etc

Two figures corresponding to the same histogram (PDF) but with very different patterns. (Lorente et al., 2021)

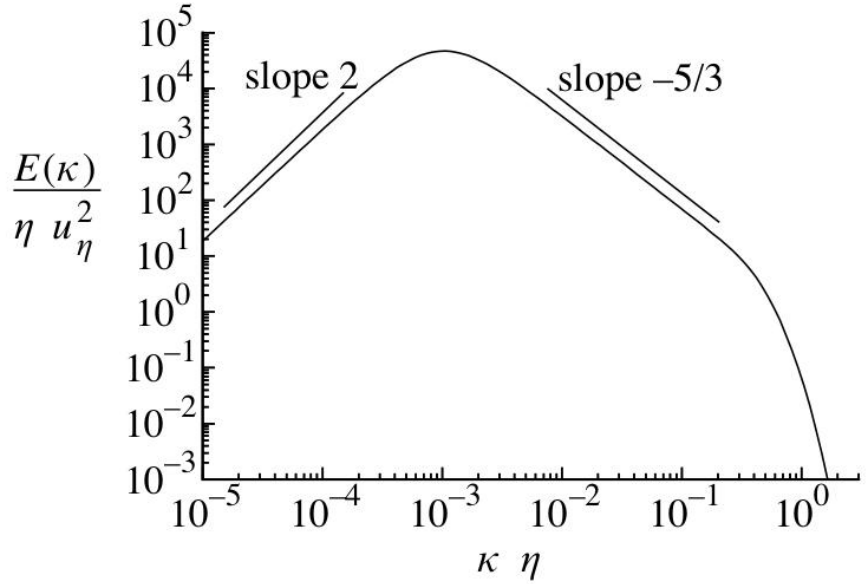


From a spectrum is hard to infer *what the flow actually looks like*.

**--> need a structural/dynamical view**

# 0. Motivations, stochastic v.s. structural views of turbulence

**The stochastic-deterministic dual nature of turbulence:**

The equations (N-S) are deterministic. But the precise prediction of instantaneous velocity fluctuation at large times is impossible, while the statistics/distributions can be determined.

**The co-existence of order and disorder:**

Discovery of *deterministic chaos*, Lorenz (1963): chaotic behavior of a set of deterministic ODEs (three-variable) obtained from a Galerkin projection of the N-S equations in a heat convection problem.

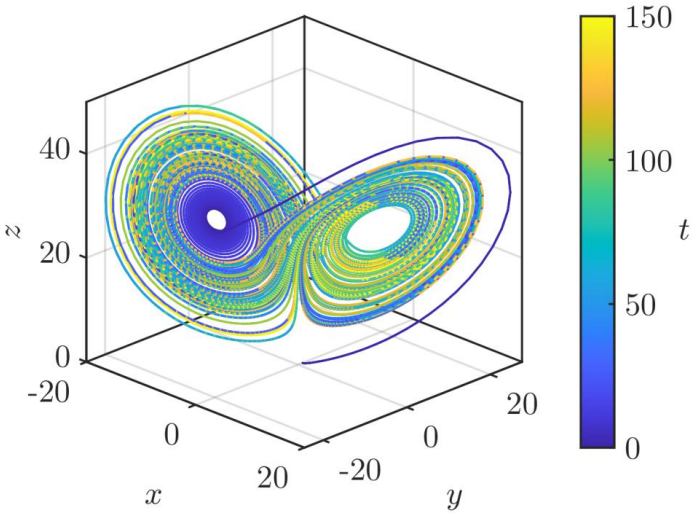


Discovery of *coherent structures* in turbulence (1970s): turbulence is not a soup of random perturbations that can only be described statistically, but contains a few large, organized objects that explain a lot about the flow.

# 1. Large-scale coherent structures

Flow

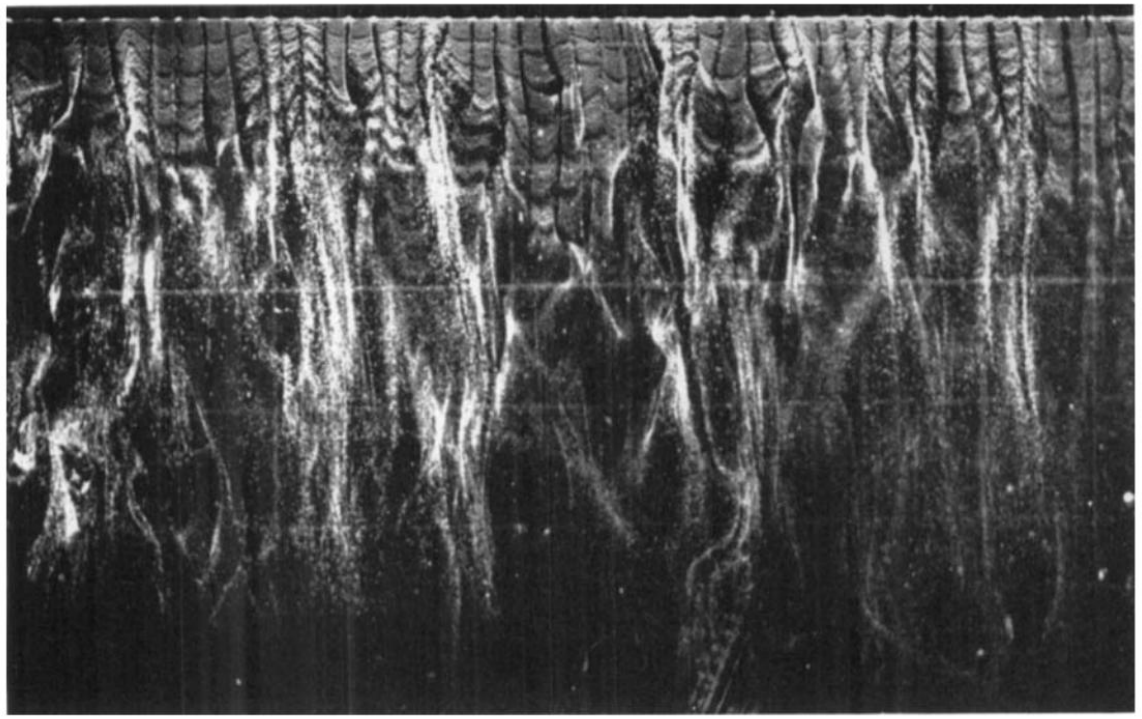

FIGURE 10c. $y^+ = 9{\cdot}6$.

**Streamwise streaks** in the buffer layer of a turbulent boundary layer (TBL). (Kline et al, 1967)

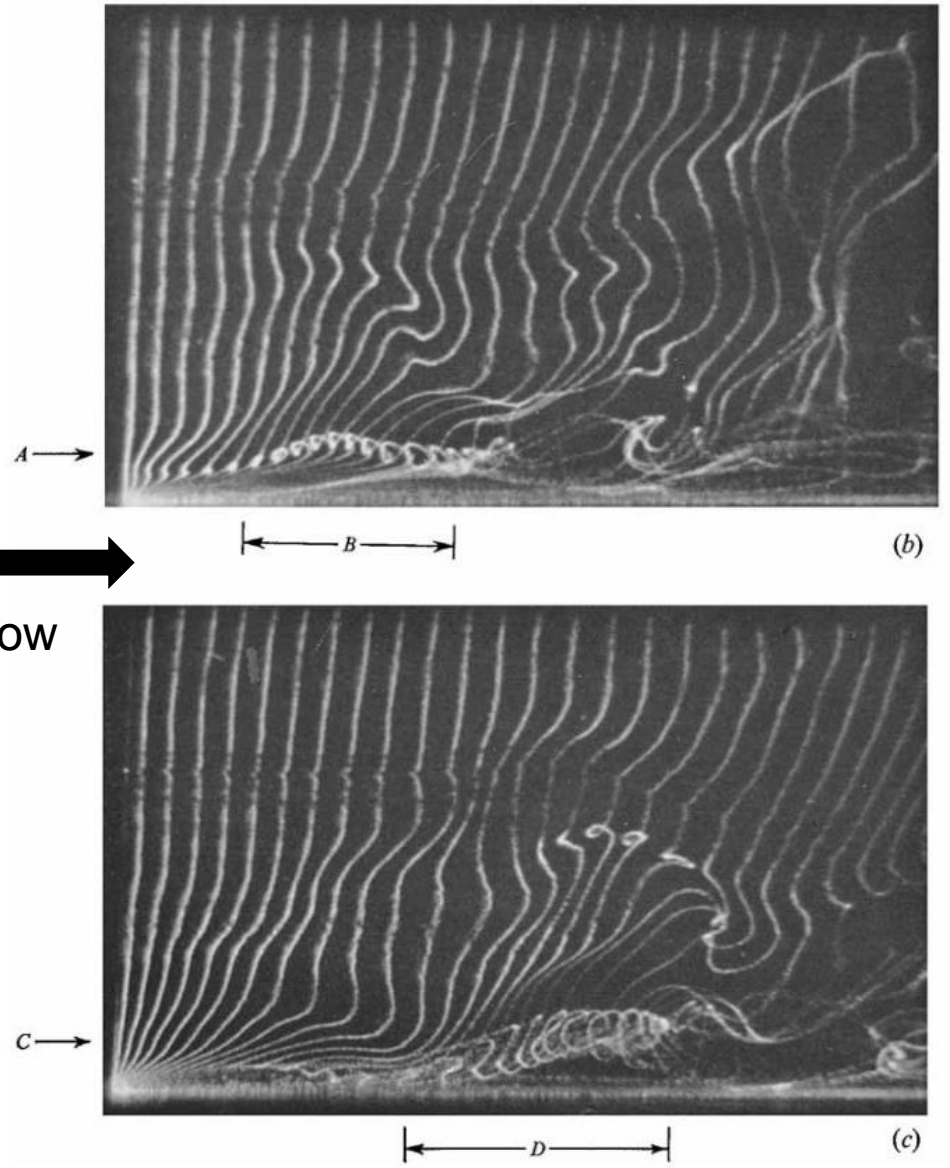


Formation of **streamwise vortex** in the buffer layer of a TBL. (Kim, Kline, & Reynolds, 1971)

# 1. Large-scale coherent structures

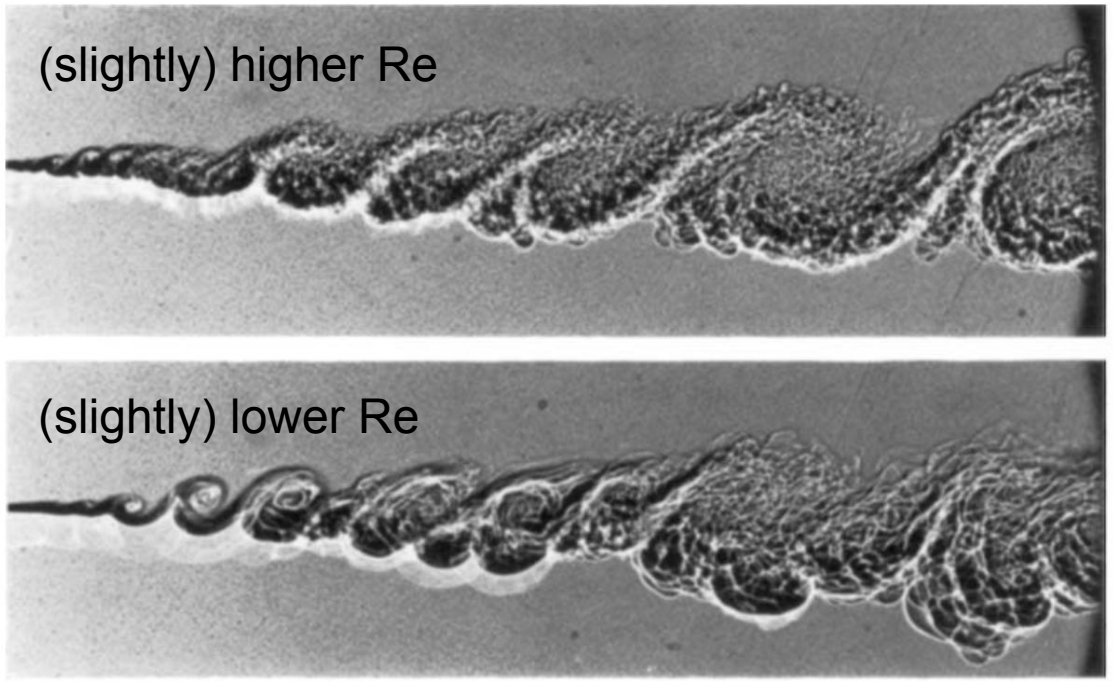


Large-scale **vortex rollers** in turbulent mixing layers.
(Brown and Roshko, 1974)

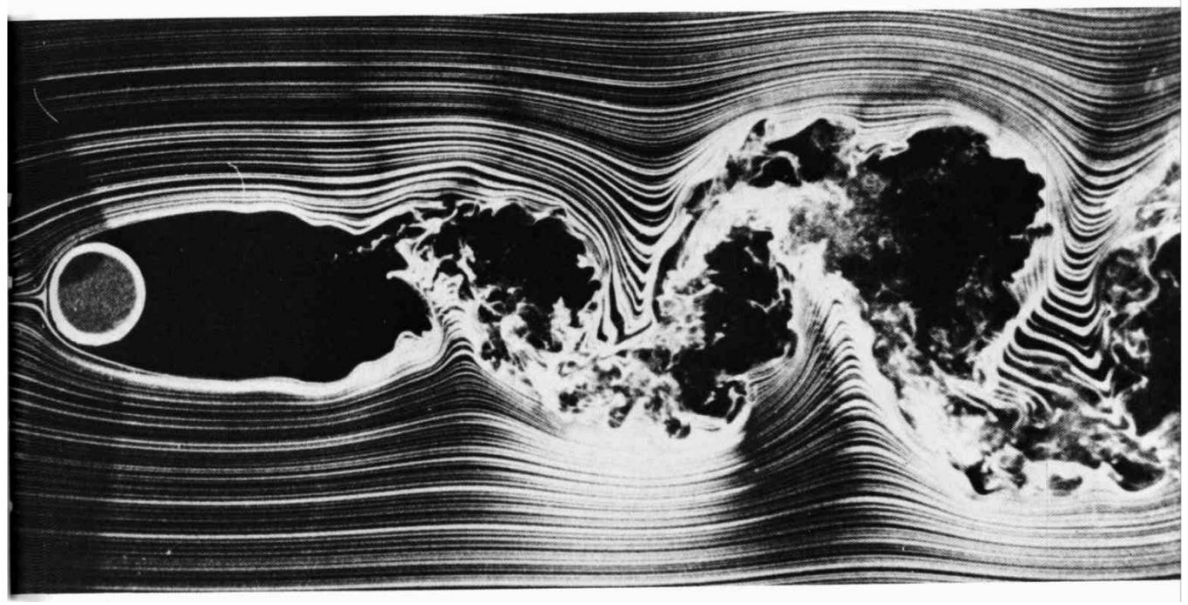

Large-scale **Kármán vortices** in a turbulent cylinder wake.
(Corke and Nagib, 1981)

- Coherent structures: (1)contain a large fraction of TKE and Reynolds stresses, (2)are unsteady, (3)typically strong enough compared to the background fluctuations to be significant/identifiable, (4)while dynamically independent enough not to be influenced by them, (5)whose evolution is relevant to the statistics of the flow.

There is no universal definition of coherent structures.
“But you know it when you see it.”

# 1.2 Coherent structures in wall-bounded turbulence

Turbulent channel at $Re_\tau = 2000$

$y^+ = 7.5$

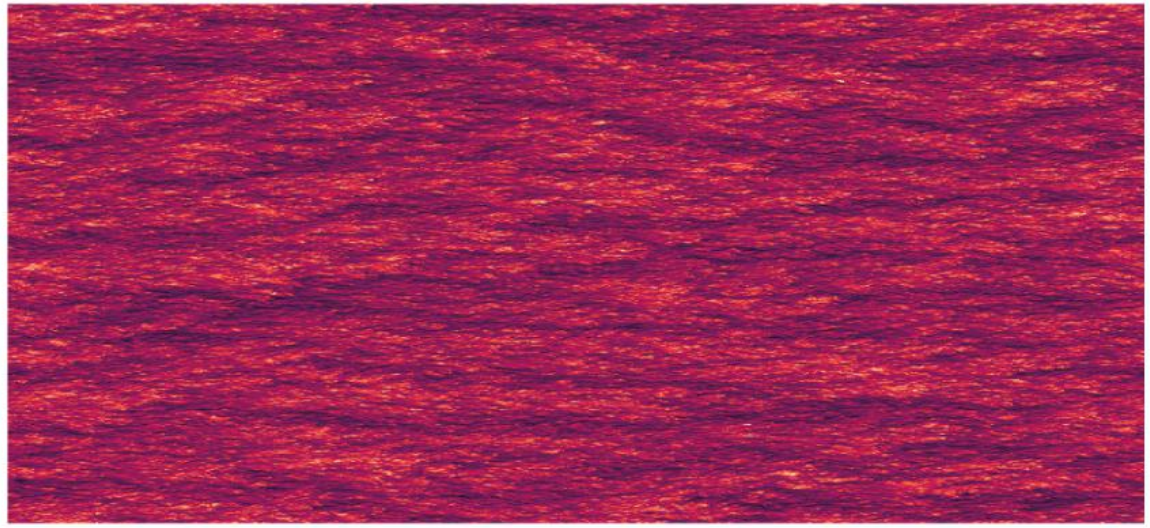

buffer layer: near wall streaks

$y/h = 0.95$

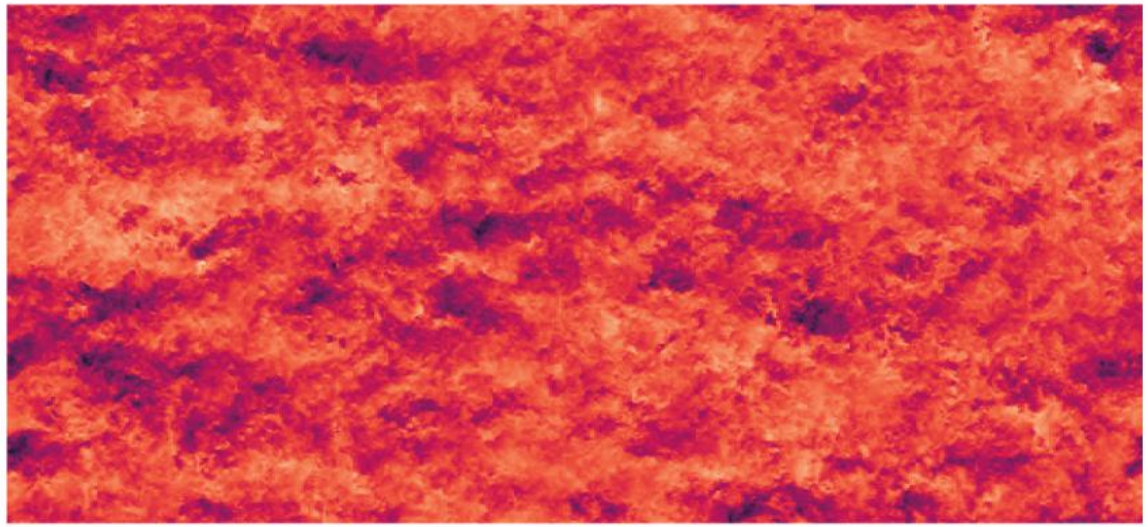

outer layer: (potentially) large-scale organized motions

# 1.2 Coherent structures in wall-bounded turbulence

(i) buffer layer structures ($5<y^+<30$, or $y^+<100$ for high-Re wall turbulence):
**near-wall streaks and streamwise vortices**

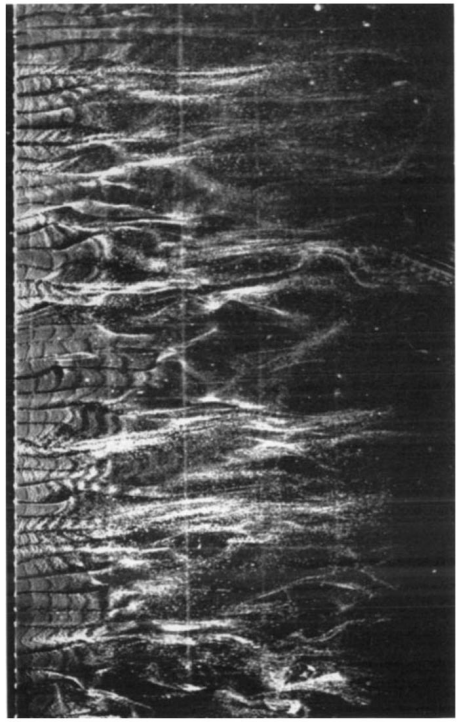

**Low-speed streaks** at $y^+=9.5$,
TBL of Kline et al. (1967)

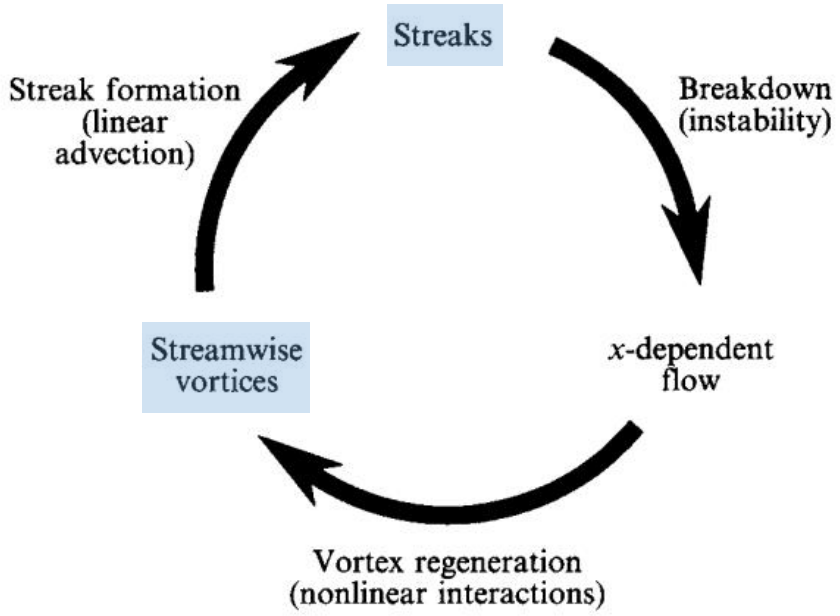


The near-wall turbulence regeneration cycle.
Hamilton, Kim, & Walaffe (1995)

scales in viscous units:
~100 $\delta_v$ wide, ~1000 $\delta_v$ long

(Pope Figs 7.33-7.34)

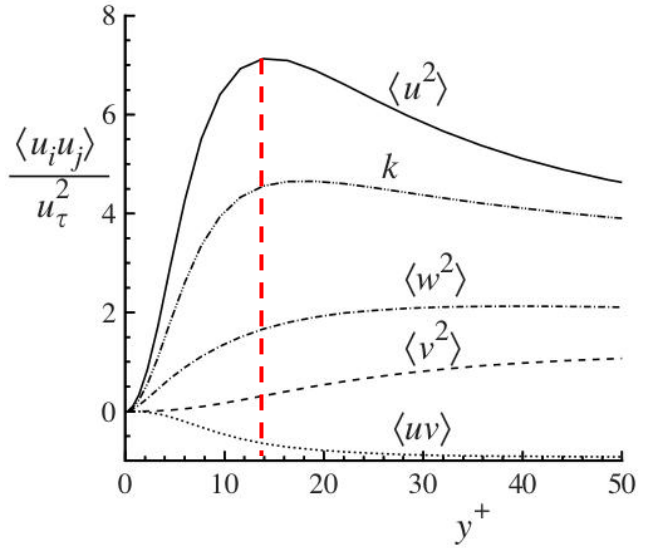


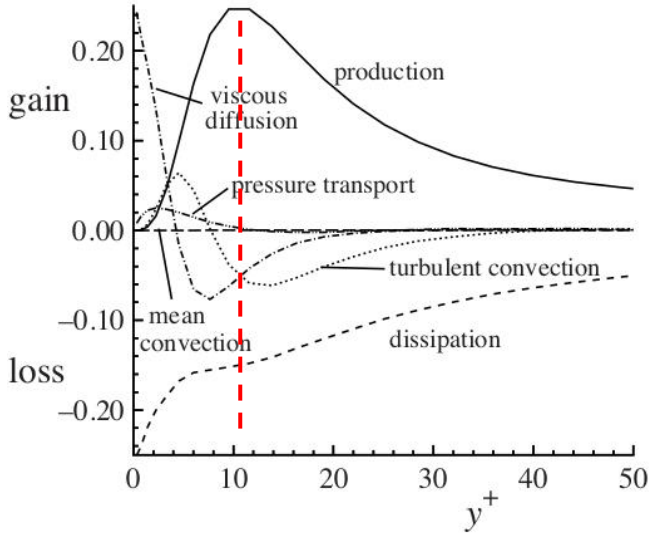


**Turbulence and its production are the most intense in the buffer layer.**

# 1.2 Coherent structures in wall-bounded turbulence

(ii) log-layer structures ($y^+>30$ & $y/h<0.3$): **quadrant events** of momentum transfer

- Events in different quadrants are not equally probable.
- Q2 and Q4 events predominate

$$P = -\overline{u'v'}\frac{\partial U}{\partial y} > 0$$

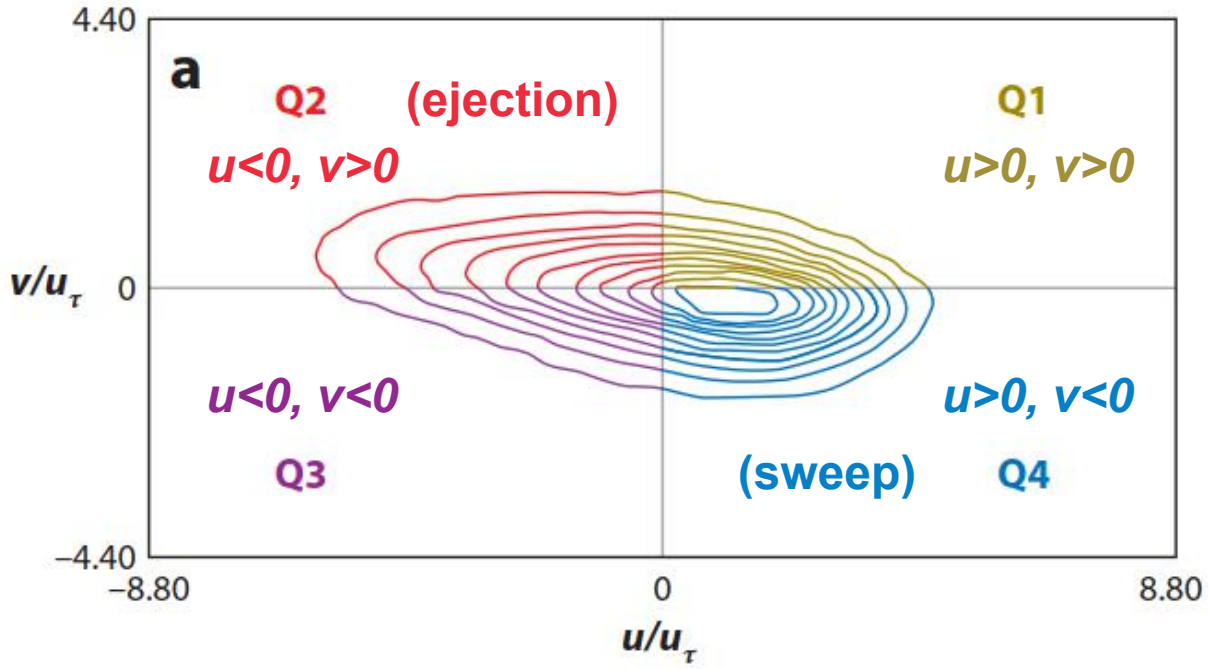


Joint PDF of fluctuation u (streamwise) and v (wall-normal)
Wallace (2016, review paper); originally Wallace & Brodkey (1977)

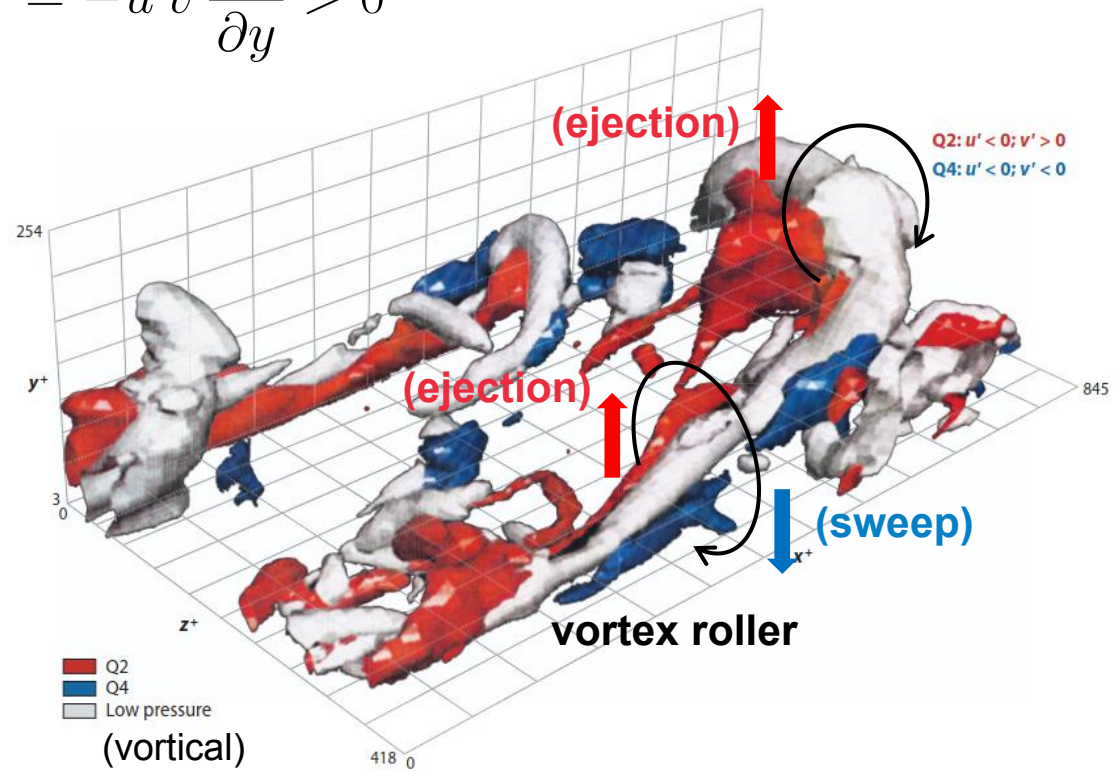


Wallace (2016); originally Robinson (1991)

# 1.2 Coherent structures in wall-bounded turbulence

(ii) log-layer structures ($y^+>30$ & $y/h<0.3$): **quadrant events** of momentum transfer

The hairpin *model*:

(Caveat: hairpins are structures of *transitional* flows.)

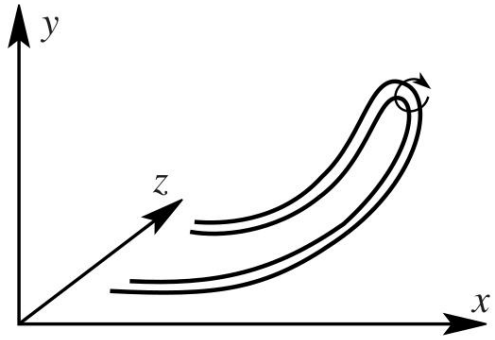


Fig. 7.43. The hairpin vortex suggested by Head and Bandyopadhyay (1981).

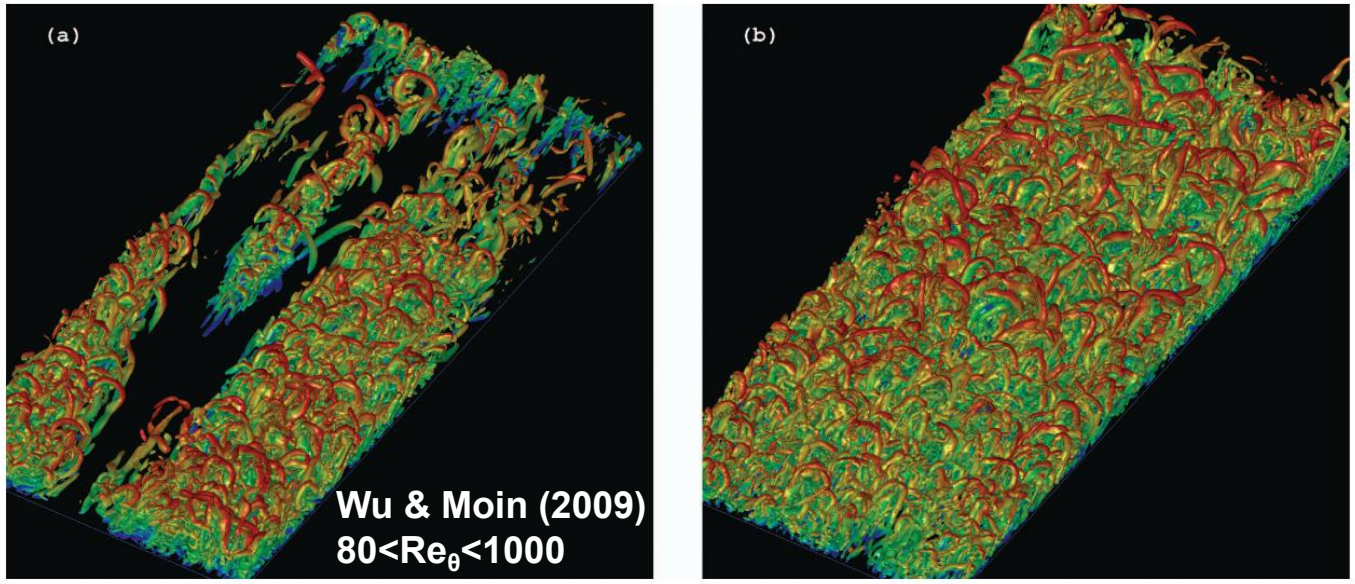


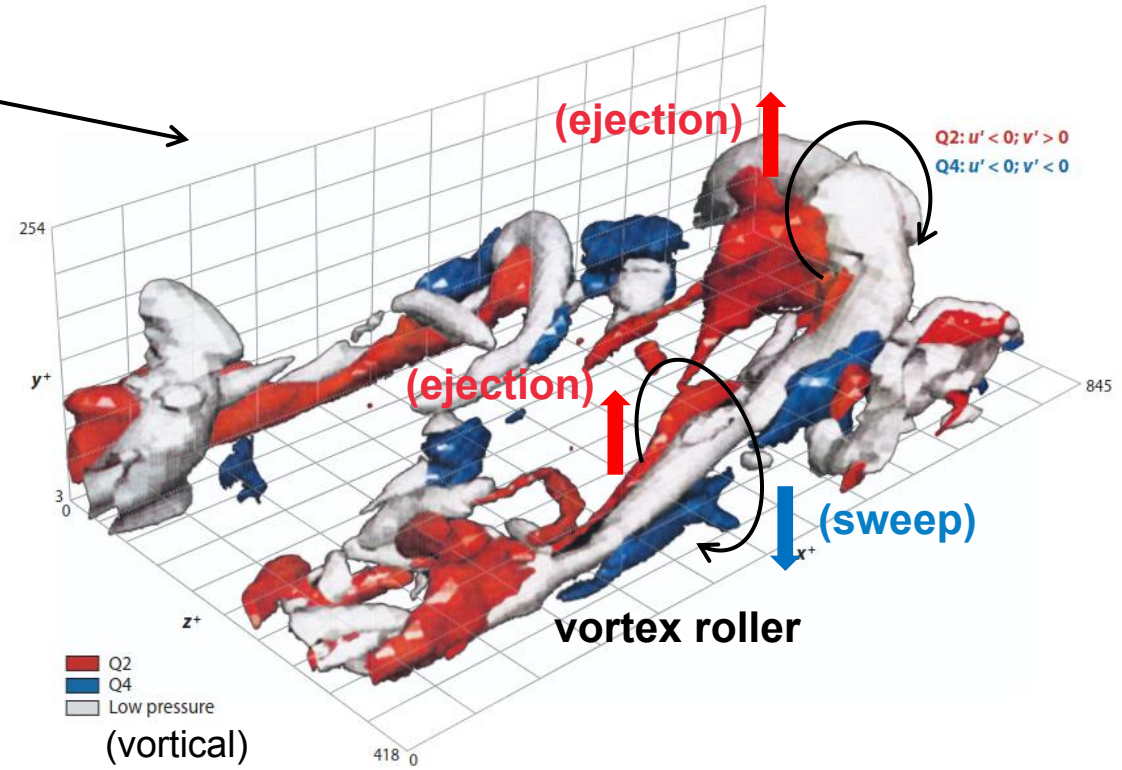


Wallace (2016); originally Robinson (1991)

# 1.2 Coherent structures in wall-bounded turbulence

(iii) outer-layer structures ($y^+>100$) **large- and very-large-scale motions**

(Adrian, 2007; Falco, 1977)

as large as the outer scale (BL thickness)

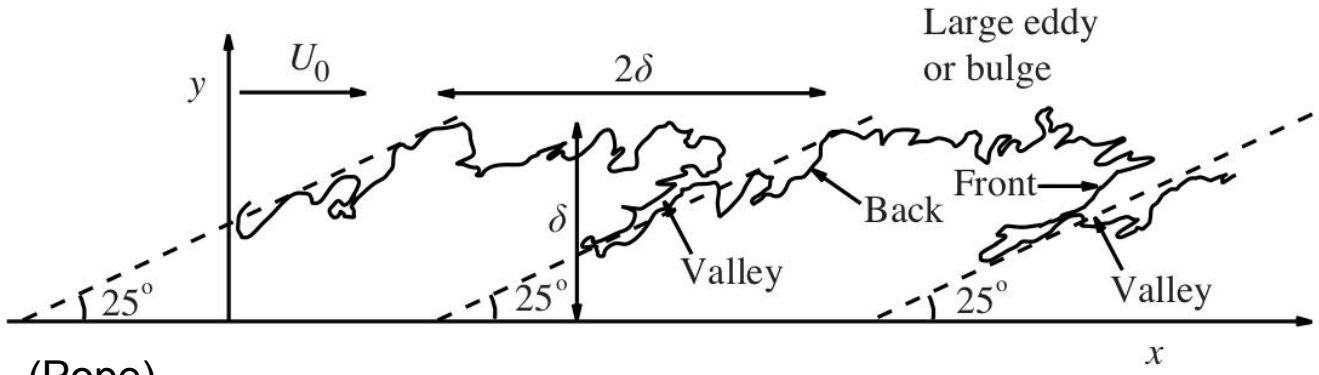


(Pope)

Fig. 7.44. The large-scale features of a turbulent boundary layer at $Re_\theta \approx 4{,}000$. The irregular line – approximating the viscous superlayer – is the boundary between smoke-filled turbulent fluid and clear free-stream fluid. (From the experiment of Falco 1977.)

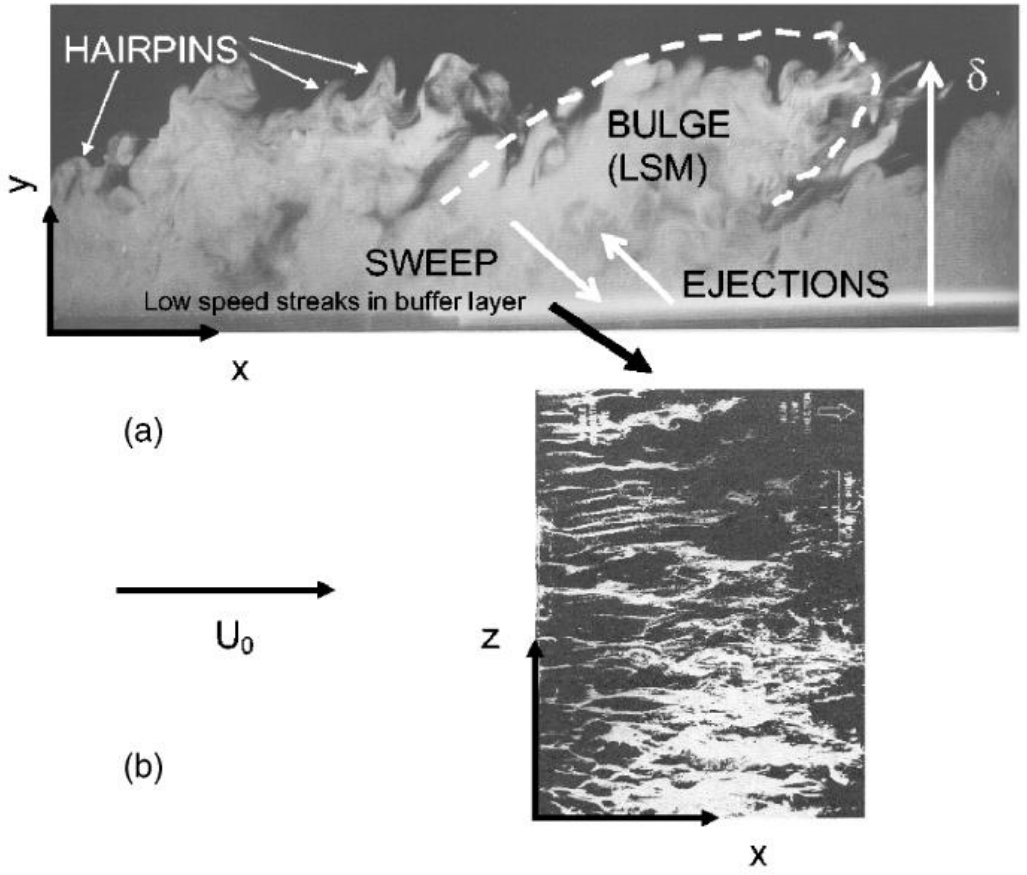

# 1.2 Coherent structures in wall-bounded turbulence

(iv) summary

**near wall region / buffer layer:**

low- and high-speed streaks (u'), streamwise vortices ($omega_x$), near-wall turbulence regeneration cycle
scale with the inner (viscous) units, ~100 $\delta_v$ wide, ~1000 $\delta_v$ long

**log layer:**

quadrant events (Q2 & Q4; u'v'): ejection & sweep pairs and associated vortex rollers
self-similar, scale with y, mostly wall-attached

**outer layer:**

large-scale and very-large-scale motions (u')
scale with the outer units (BL thickness, channel half width), O(2-3$\delta$) for LSM and O(10$\delta$) for VLSM

# 2. Geometry of small-scale turbulence

Small-scale turbulence is **not completely random**; it has certain geometries, featuring **vortex tubes** and **rate-of-strain sheets**.

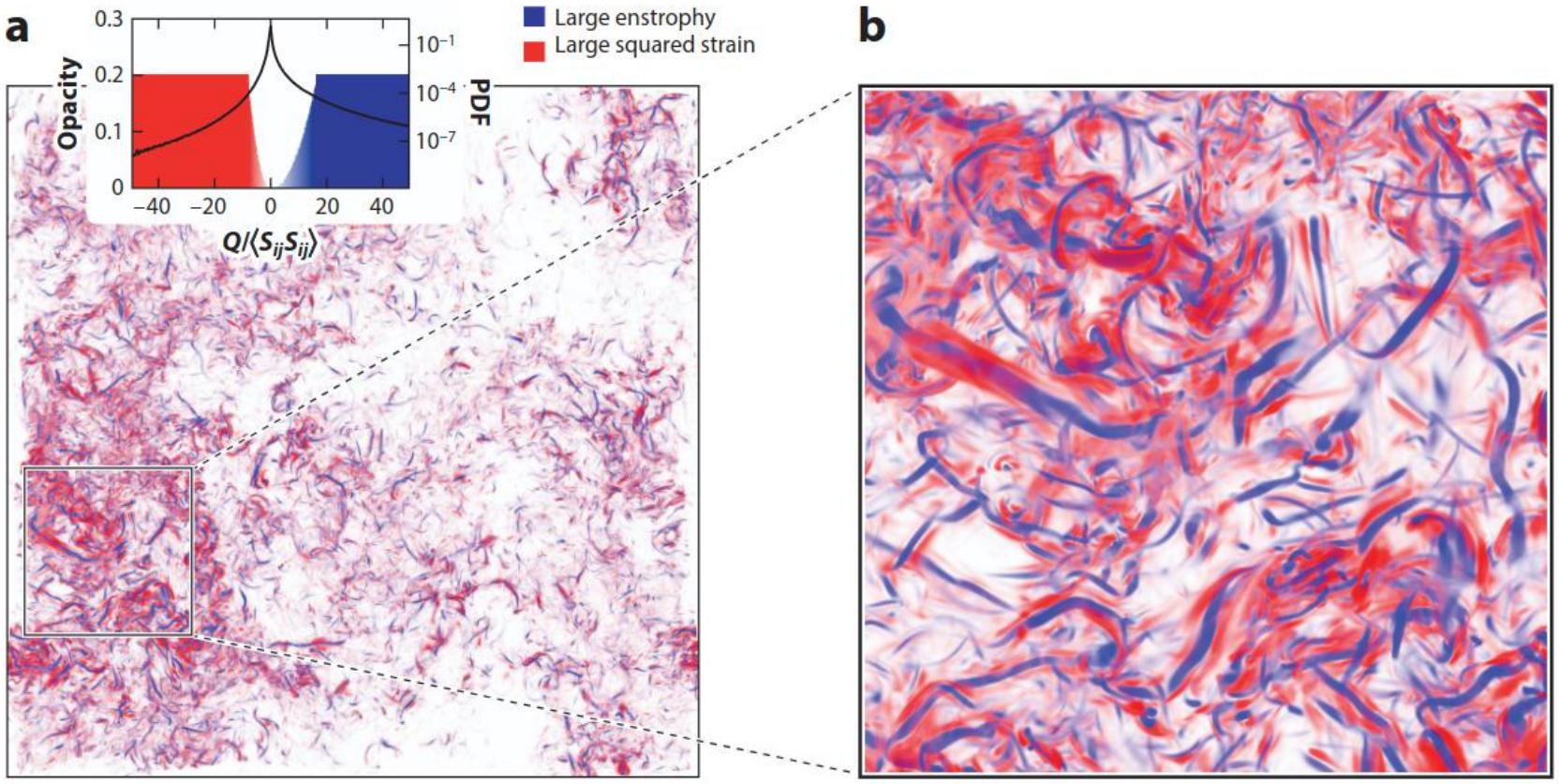


**Figure 2**

(*a*) Visualization of large enstrophy (*blue*) and large squared strain (*red*) by means of the second invariant $Q$ from a simulation of homogeneous isotropic turbulence ($Re_\lambda \approx 280$). (*b*) Zoomed-in view of the boxed region in panel *a*. Since these strong events are spatially colocalized, their contribution to the pressure partially cancels (Equation 10). Abbreviation: PDF, probability density function. Figure provided by Cristian C. Lalescu.

(Johnson and Wilczek, 2022)

# 2. Geometry of small-scale turbulence

**Motivation:**

There are limitations of vorticity/enstrophy in identifying the strongly vortical/swirling regions.
Vorticity is neither an essential nor a necessary condition for the existence of swirling motion.

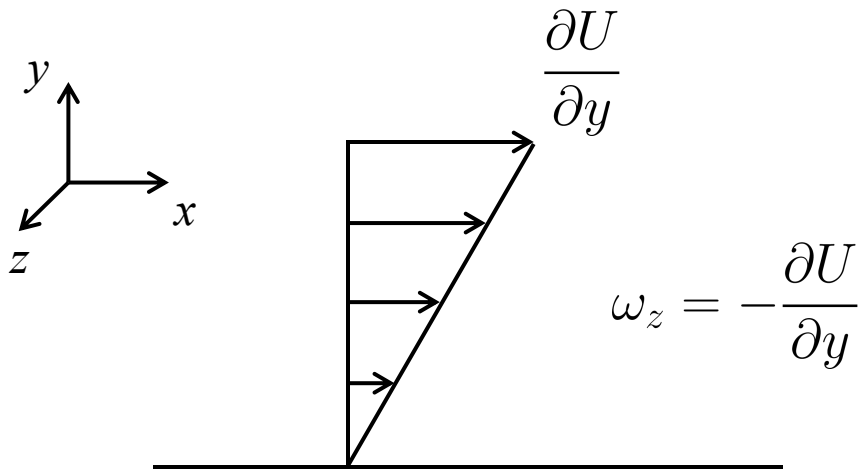


$$\omega_z = -\frac{\partial U}{\partial y}$$

Laminar shear flow.
(Nonzero vorticity, no vortices.)

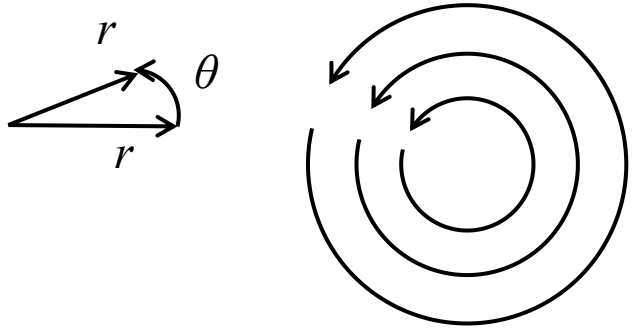


$$u_\theta = \frac{\Gamma}{2\pi r}$$

$$\omega_z = \frac{u_\theta}{r} + \frac{\partial u_\theta}{\partial r} = 0$$

Potential vortex.
(No vorticity.)

--> need criteria based on the invariants of the velocity gradient tensor

# 2. Geometry of small-scale turbulence

The velocity gradient tensor (VGT): $a_{ij} = \dfrac{\partial u_i}{\partial x_j}$ $\quad \boldsymbol{A} = \begin{bmatrix} a_{11} & a_{12} & a_{13} \\ a_{21} & a_{22} & a_{23} \\ a_{31} & a_{32} & a_{33} \end{bmatrix}$

Characteristic polynomial (real-coefficient, third order):

$$\det(\lambda \boldsymbol{I} - \boldsymbol{A}) = \begin{vmatrix} \lambda - a_{11} & -a_{12} & -a_{13} \\ -a_{21} & \lambda - a_{22} & -a_{23} \\ -a_{31} & -a_{32} & \lambda - a_{33} \end{vmatrix} = \lambda^3 - I_1\lambda^2 + I_2\lambda - I_3 = 0$$

Principal invariants:
(independent of coordinate system)

$$\begin{aligned} I_1 &= a_{11} + a_{22} + a_{33} \\ &= \mathrm{tr}(\boldsymbol{A}) \\ &= a_{ii} \\ I_2 &= a_{11}a_{22} + a_{22}a_{33} + a_{33}a_{11} - a_{12}a_{21} - a_{23}a_{32} - a_{13}a_{31} \\ &= \frac{\mathrm{tr}(\boldsymbol{A})^2 - \mathrm{tr}(\boldsymbol{A}^2)}{2} \\ &= \frac{1}{2}((a_{ii})^2 - a_{ij}a_{ji}) \\ I_3 &= a_{11}(a_{22}a_{33} - a_{23}a_{32}) - a_{12}(a_{21}a_{33} - a_{23}a_{31}) + a_{13}(a_{21}a_{32} - a_{22}a_{31}) \\ &= \det(\boldsymbol{A}) \end{aligned}$$

$$\begin{aligned} &\lambda^3 - P\lambda^2 + Q\lambda - R = 0, \\ &P = \mathrm{tr}(A) = a_{ii} = 0 \\ &Q = -\frac{1}{2}a_{ij}a_{ji} \\ &R = \det(A) \end{aligned}$$

# 2. Geometry of small-scale turbulence

The velocity gradient tensor (VGT): $a_{ij} = \frac{\partial u_i}{\partial x_j}$ $\boldsymbol{A} = \begin{bmatrix} a_{11} & a_{12} & a_{13} \\ a_{21} & a_{22} & a_{23} \\ a_{31} & a_{32} & a_{33} \end{bmatrix}$

Characteristic polynomial (real-coefficient, third order):

$$\lambda^3 - P\lambda^2 + Q\lambda - R = 0,$$
$$P = \mathrm{tr}(A) = a_{ii} = 0$$
$$Q = -\frac{1}{2} a_{ij} a_{ji}$$
$$R = \det(A)$$

(incompressibility)

**Criterion 1. The Q-criterion** (second invariant of the VGT) $Q = -\frac{1}{2}\frac{\partial u_i}{\partial x_j}\frac{\partial u_j}{\partial x_i}$ (Hunt, Wray, and Moin, 1988)

Relation to the Pressure Poisson: $\frac{1}{\rho}\nabla^2 p = -\frac{\partial u_i}{\partial x_j}\frac{\partial u_j}{\partial x_i} = 2Q$

**Q>0 --> there is very likely a local pressure minimum (vortex core)**

# 2. Geometry of small-scale turbulence

**Criterion 1. The Q-criterion** (second invariant of the VGT) $Q = -\frac{1}{2}\frac{\partial u_i}{\partial x_j}\frac{\partial u_j}{\partial x_i}$ (Hunt, Wray, and Moin, 1988)

Relation to the Pressure Poisson: $\frac{1}{\rho}\nabla^2 p = -\frac{\partial u_i}{\partial x_j}\frac{\partial u_j}{\partial x_i} = 2Q$

**Q>0 --> there is very likely a local pressure minimum (possible vortex core)**

Another interpretation: $Q = -\frac{1}{2}\frac{\partial u_i}{\partial x_j}\frac{\partial u_j}{\partial x_i} = \frac{1}{2}\left(\Omega_{ij}\Omega_{ij} - S_{ij}S_{ij}\right) = \frac{1}{2}[\|\Omega\|^2 - \|S\|^2]$

**Q>0 --> rotation dominates strain --> swirling motion**

---

Example.

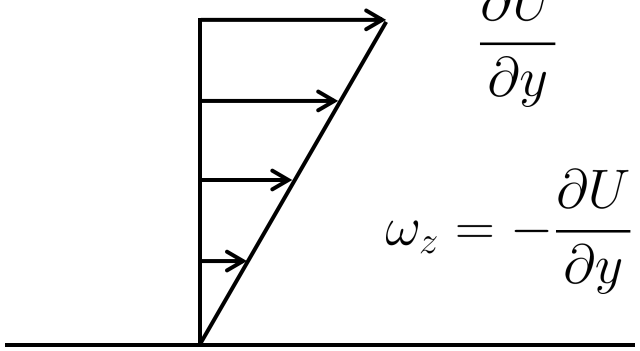


$$S = \frac{1}{2}\begin{pmatrix} 0 & \frac{dU}{dy} & 0 \\ \frac{dU}{dy} & 0 & 0 \\ 0 & 0 & 0 \end{pmatrix}, \qquad \Omega = \frac{1}{2}\begin{pmatrix} 0 & \frac{dU}{dy} & 0 \\ -\frac{dU}{dy} & 0 & 0 \\ 0 & 0 & 0 \end{pmatrix}$$

$$Q = \frac{1}{2}[\|\Omega\|^2 - \|S\|^2] = 0$$

**(Q=0, where Q excludes the contribution of pure strain/shear to vorticity.)**

# 2. Geometry of small-scale turbulence

The velocity gradient tensor (VGT): $a_{ij} = \dfrac{\partial u_i}{\partial x_j}$

$$\boldsymbol{A} = \begin{bmatrix} a_{11} & a_{12} & a_{13} \\ a_{21} & a_{22} & a_{23} \\ a_{31} & a_{32} & a_{33} \end{bmatrix}$$

Characteristic polynomial (real-coefficient, third order):

$$\lambda^3 - P\lambda^2 + Q\lambda - R = 0,$$
$$P = \mathrm{tr}(A) = a_{ii} = 0 \quad \text{(incompressibility)}$$
$$Q = -\frac{1}{2} a_{ij} a_{ji}$$
$$R = \det(A)$$

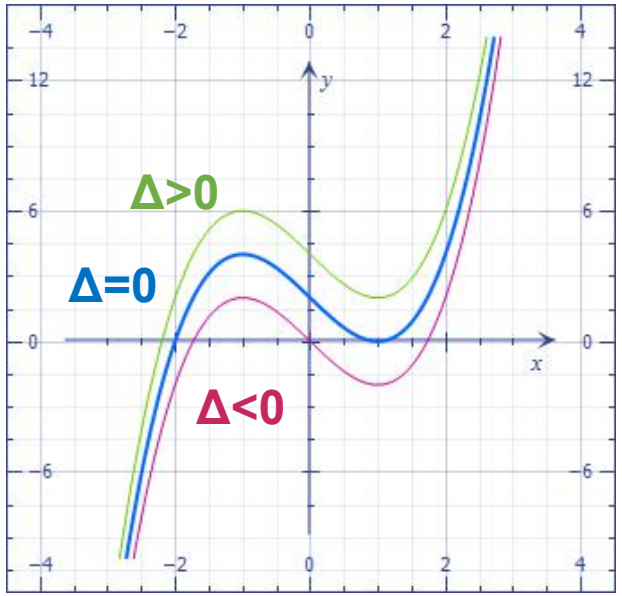


(cases with 1, 2, and 3 real roots of a 'depressed' cubic)

Incompressible, reduces to: $\lambda^3 + Q\lambda - R = 0$

('depressed' cubic equation)

**Criterion 2. The Δ-discriminant**

$$\triangle = \left(\frac{1}{3}Q\right)^3 + \left(\frac{1}{2}R\right)^2$$

- all real coefficients: real roots or complex conjugate complex roots (must be in pairs), according to the Fundamental Theorem of Algebra
- possible cases of roots (eigenvalues, EVs): **3 real (Δ<0, pure straining)** OR **1 real + 2 complex conjugate (Δ>0, swirling)**

**Δ>0, complex EVs, swirling region**

(Chong, Perry, Cantwell, 1990)

# 2. Geometry of small-scale turbulence

Incompressible, reduces to: $\lambda^3 + Q\lambda - R = 0$

('depressed' cubic equation)

**Criterion 2. The Δ-discriminant**

$$\triangle = \left(\frac{1}{3}Q\right)^3 + \left(\frac{1}{2}R\right)^2$$

- all real coefficients: real roots or complex conjugate roots (must be in pairs), according to the Fundamental Theorem of Algebra.
- possible cases of roots (eigenvalues, EVs): **3 real (Δ<0, pure strain-like)** OR **1 real + 2 complex conjugate (Δ>0, swirling)**

**Δ>0, complex EVs, swirling region**

(Chong, Perry, Cantwell, 1990)

Incompressibility: $P = a_{ii} = \lambda_1 + \lambda_2 + \lambda_3 = 0$

**Δ<0, 3 real EVs, pure strain-like**

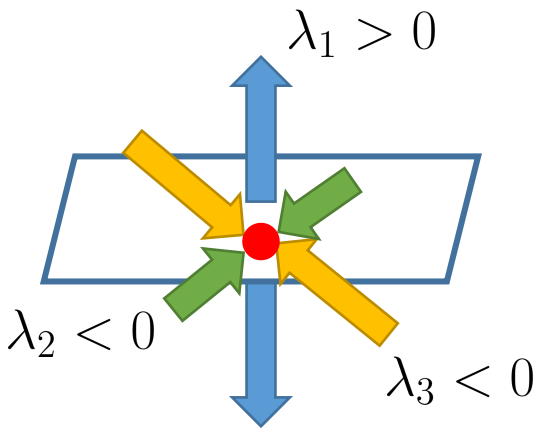


(tube-like straining)

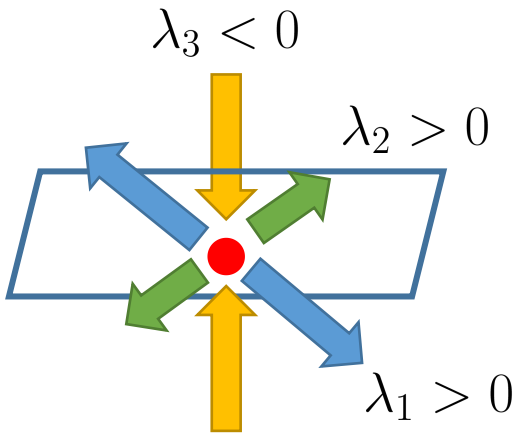


(sheet-line straining)

**Δ>0, 1 real + 2 complex EVs, swirling**

$\lambda_2^* = \lambda_3$

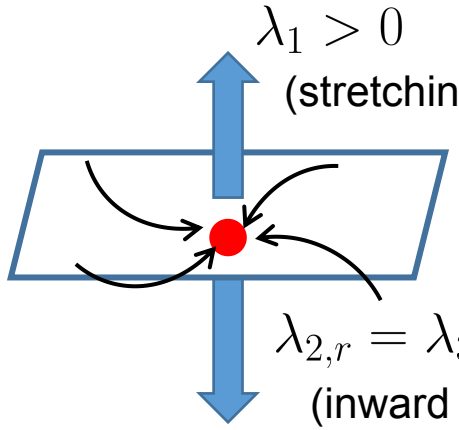


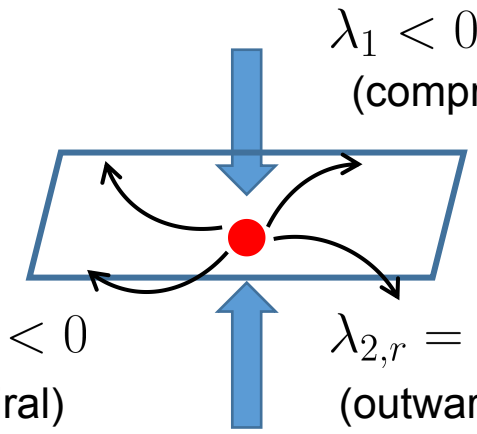


(eigenvector orthogonality is not assumed)

# 2. Geometry of small-scale turbulence

Incompressible, reduces to: $\lambda^3 + Q\lambda - R = 0$

('depressed' cubic equation)

$$a_{ij} = \frac{\partial u_i}{\partial x_j}$$

$$\boldsymbol{A} = \begin{bmatrix} a_{11} & a_{12} & a_{13} \\ a_{21} & a_{22} & a_{23} \\ a_{31} & a_{32} & a_{33} \end{bmatrix}$$

In the case of **Δ>0, 1 real + 2 complex conjugate EVs**, what quantifies the swirling strength?

The complex diagonalization of A: (a similarity transformation)

$$A = P \begin{bmatrix} \lambda_r & & \\ & \lambda_{cr} & \lambda_{ci} \\ & -\lambda_{ci} & \lambda_{cr} \end{bmatrix} P^{-1}$$

$$\lambda_1 = \lambda_r$$

$$\lambda_{2,3} = \lambda_{cr} \pm \mathrm{i}\lambda_{ci}$$

stretching/compressing — rotation

**Criterion 3. The $\lambda_{ci}$-criterion (imaginary part of the complex EV)**

Zhou, Adrian et al. (1999)

**Δ>0, 1 real + 2 complex EVs, swirling**

$$\lambda_2^* = \lambda_3$$

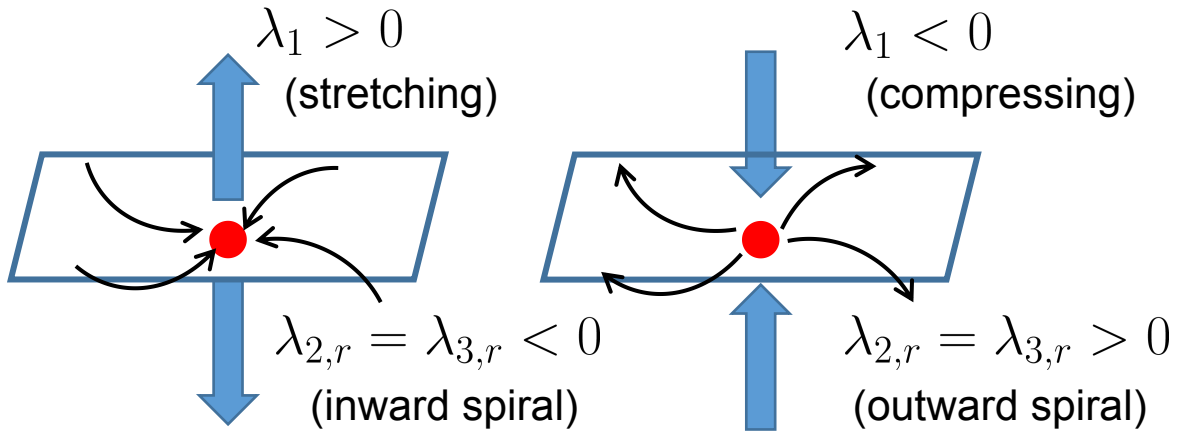


(eigenvector orthogonality is not assumed)

# 2. Geometry of small-scale turbulence

isotropic turbulence of $Re_\lambda$=164

Summary and applications.

**Criterion 1. The Q-criterion, Q>0**
**(second invariant of the VGT)**
Hunt, Wray, and Moin (1988)

**Criterion 2. The Δ-discriminant (of the VGT), Δ>0**
Chong, Perry, and Cantwell (1990)

**Criterion 3. The $\lambda_{ci}$-criterion, $|\lambda_{ci}|>0$**
**(imaginary part of the complex EV of the VGT)**
Zhou, Adrian et al. (1999)

**Criterion 4. The $\lambda_2$-criterion, $\lambda_2<0$**
**(second EV of $S^2+\Omega^2$)**
Jeong & Hussain (1995) - read the paper for the math

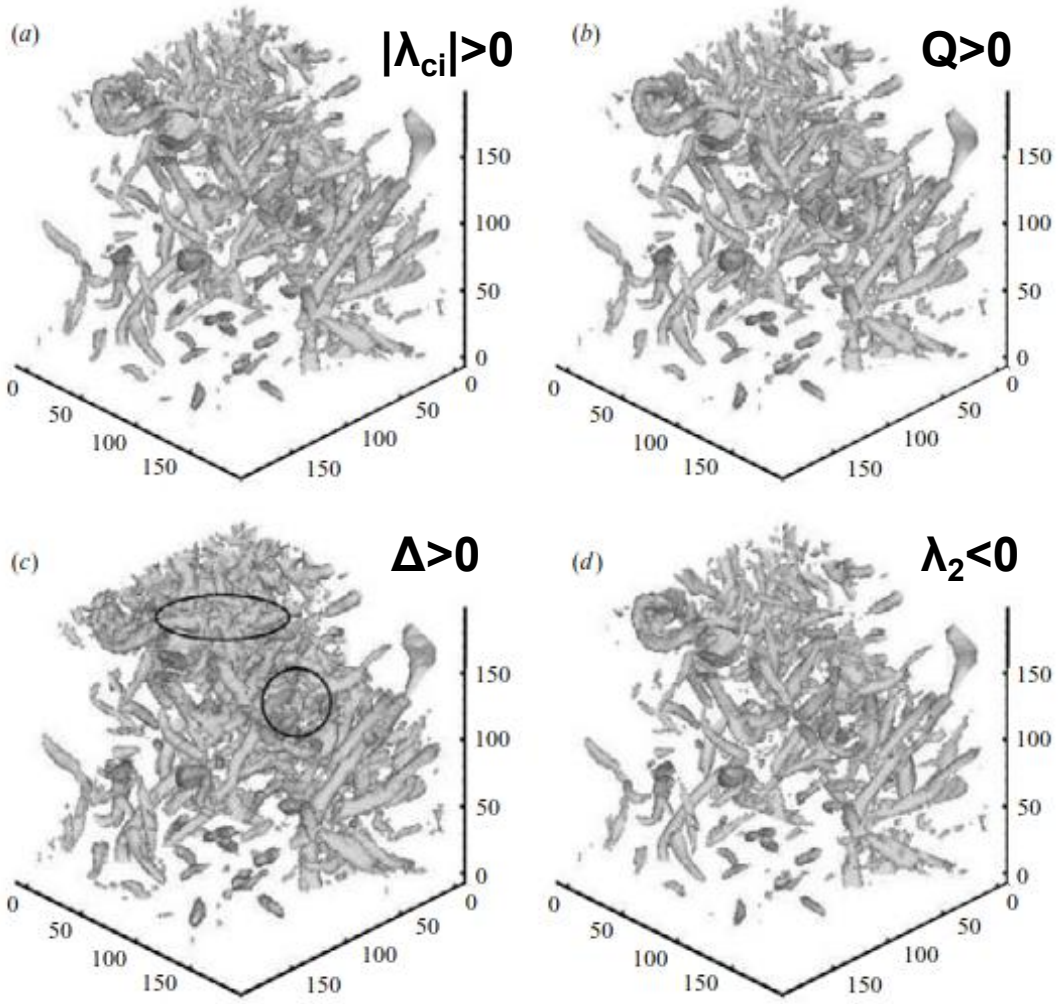


(Chakraborty et al, 2005)

- They all give quite similar results. Need a bit of thresholding.

# 3. Data-driven coherent structure eduction

Motivations: the equivalent representations of turbulence in **physical** and **spectral** spaces

Fourier spectrum at kappa: the energy density of eddies of size L~2*pi/kappa

spectral space: wavenumber kappa

physical space: length scale L

3D periodic box turbulence

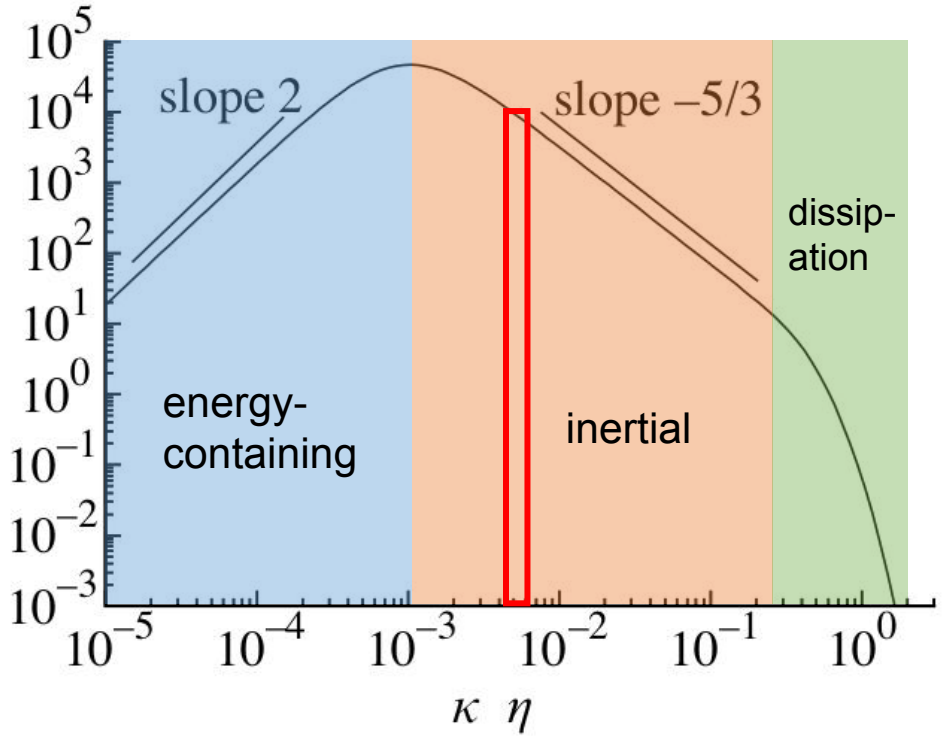


Pope Fig. 6.13

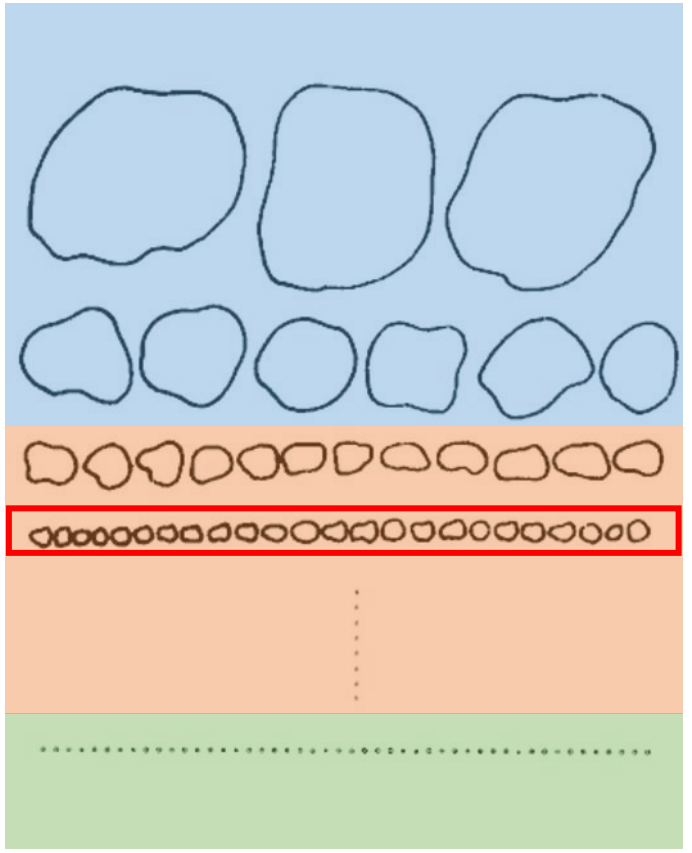

# 3. Data-driven coherent structure eduction

Motivations: the equivalent representations of turbulence in **physical** and **spectral** spaces
Fourier spectrum at kappa: the energy density of eddies of size L~2*pi/kappa

3D periodic box turbulence

spectral space: wavenumber kappa

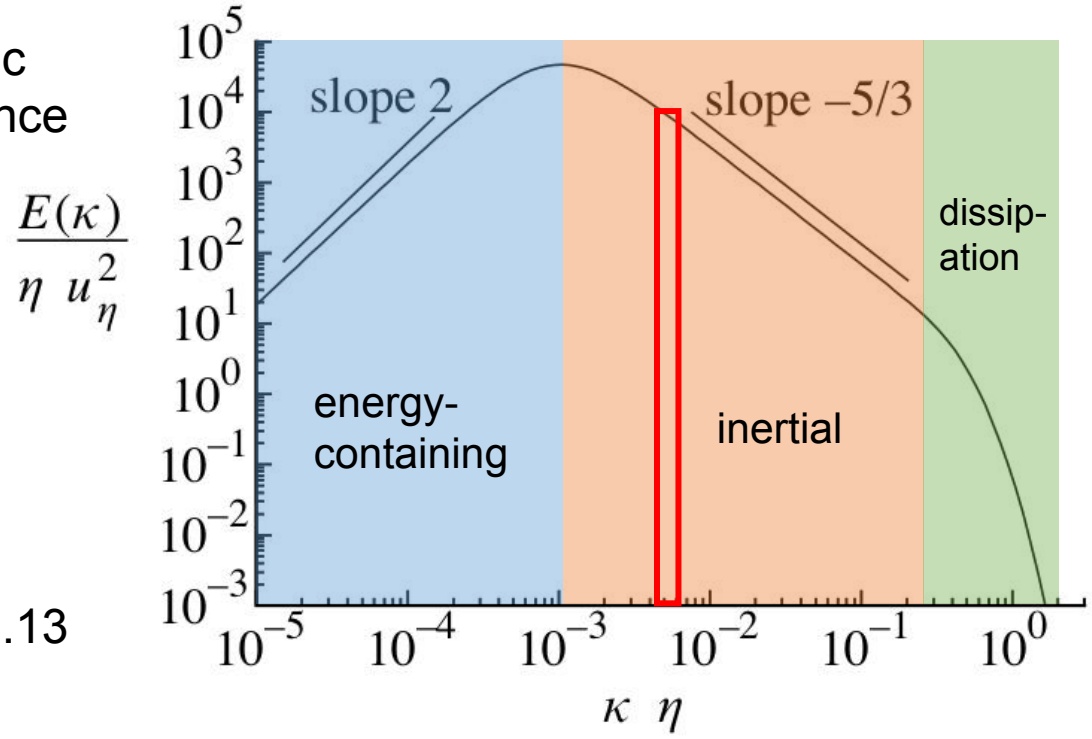


Pope Fig. 6.13

Fourier expansion in periodic directions:
(with eigenfunctions being sine and cosine waves)

$$u_i(\boldsymbol{x},t) = \sum_{\kappa_x}\sum_{\kappa_y}\sum_{\kappa_z} \hat{u}_i(\boldsymbol{\kappa},t) e^{\mathrm{i}\kappa_x x} e^{\mathrm{i}\kappa_y y} e^{\mathrm{i}\kappa_z z}$$

$$\hat{u}_i(\boldsymbol{\kappa},t) = \mathcal{F}[u_i(\boldsymbol{x},t)]$$

expansion coefficients

orthogonal eigenfunctions (waves)

$$E(\boldsymbol{\kappa}) = \frac{1}{2}\langle \hat{u}_i(\boldsymbol{\kappa},t)\hat{u}_i^*(\boldsymbol{\kappa},t)\rangle$$

ensemble average of expansion coefficients
--> energy spectrum, indicating the relative magnitudes of different eigenfunctions (waves at different wavenumbers)

--> What to do in inhomogeneous directions which we cannot Fourier-expand?

# 3. Data-driven coherent structure eduction

The idea of the proper orthogonal decomposition (POD):

(Lumley 1967, 1970)

$$u(\boldsymbol{x},t) = \sum_n a_n(t)\underbrace{\phi_n(\boldsymbol{x})}_{\text{orthogonal eigenfunctions ('coherent structures')}}$$

$a_n(t)$: expansion coefficients

- works in aperiodic directions
- eigenfunctions are
  - empirical / based-on data / flow-dependent
  - sorted by the modal index n
  - orthogonal and normalized

$$\underbrace{\langle \phi_n, \phi_m \rangle_L}_{\text{inner-product (over which orthogonality is defined)}} = \frac{1}{L^3}\int_0^L\int_0^L\int_0^L \phi_n(\boldsymbol{x})\phi_m(\boldsymbol{x})\,\mathrm{d}\boldsymbol{x} = \delta_{m,n}$$

Fourier expansion:

$$u_i(\boldsymbol{x},t) = \sum_{\kappa_x}\sum_{\kappa_y}\sum_{\kappa_z} \underbrace{\hat{u}_i(\boldsymbol{\kappa},t)}_{\text{expansion coefficients}} \underbrace{e^{\mathrm{i}\kappa_x x}e^{\mathrm{i}\kappa_y y}e^{\mathrm{i}\kappa_z z}}_{\text{orthogonal eigenfunctions (waves)}}$$

$$\hat{u}_i(\boldsymbol{\kappa},t) = \mathcal{F}[u_i(\boldsymbol{x},t)]$$

- works in periodic directions
- eigenfunctions are
  - analytical
  - sorted by the wavenumber kappa
  - orthogonal and normalized

$$\underbrace{\langle e^{\mathrm{i}\kappa_x}, e^{-\mathrm{i}\kappa'_x} \rangle_L}_{\text{inner-product}} = \frac{1}{L}\int_0^L e^{\mathrm{i}\kappa_x}e^{-\mathrm{i}\kappa'_x}\,\mathrm{d}x = \delta_{\kappa_x,\kappa'_x}$$

(Fourier modes at different wavenumbers are mutually orthogonal.)

# 3. Data-driven coherent structure eduction

The idea of the proper orthogonal decomposition (POD):

(Lumley 1967, 1970)

$$u(\boldsymbol{x},t) = \sum_n a_n(t)\phi_n(\boldsymbol{x}) \qquad \langle \phi_n, \phi_m \rangle_L = \frac{1}{L^3}\int_0^L\int_0^L\int_0^L \phi_n(\boldsymbol{x})\phi_m(\boldsymbol{x})\,\mathrm{d}\boldsymbol{x} = \delta_{m,n}$$

expansion coefficients

orthogonal eigenfunctions ('coherent structures')

inner-product (over which the orthogonality is defined)

The POD eigenvalue problem (a Fredholm eigenvalue problem) in 1-D, in search of **orthogonal modes phi$_n$(x)**

$$\frac{1}{L}\int_0^L R_{uu}(x_1,x_1')\phi_n(x_1')\,\mathrm{d}x_1' = \lambda_n\phi_n(x_1)$$ - n is the eigenvalue index (mode index)

$$R_{uu}(x_1,x_1') = \langle u(x_1)u(x_1')\rangle$$ - two-point correlation tensor in 1-D, **real symmetric**

The POD expansion: $u(x,t) = \sum_n a_n(t)\phi_n(x) \quad E = \frac{(1/L)\int_0^L \langle u^2\rangle\,\mathrm{d}x}{2} = \frac{1}{2}\sum_n \langle a_n^2(t)\rangle, E(n) = \frac{1}{2}\langle a_n^2(t)\rangle = \frac{\lambda_n}{2}$

eigen-spectrum (energy in each mode)

The expansion coefficients (via orthogonal projection): $a_n(t) = \frac{1}{L}\int_0^L u(x,t)\phi_n(x)\,\mathrm{d}x$

(instantaneous flow field projected on eigenfunctions)

# 3. Data-driven coherent structure eduction

The POD eigenvalue problem (a Fredholm eigenvalue problem) in 1-D, in search of **orthogonal modes phi$_n$(x)**

$$\frac{1}{L}\int_0^L R_{uu}(x_1, x_1')\phi_n(x_1')\,\mathrm{d}x_1' = \lambda_n \phi_n(x_1)$$ - n is the eigenvalue index (mode index)

$$R_{uu}(x_1, x_1') = \langle u(x_1)u(x_1')\rangle$$ - two-point correlation tensor in 1-D, **real symmetric**

Numerical procedures of POD: (assume a general flow quantity ***q*** of zero mean)

(1) collect snapshots: $\boldsymbol{Q} = [\boldsymbol{q}_1, \boldsymbol{q}_2, \cdots, \boldsymbol{q}_{N_t}] \in \mathbb{R}^{N_d \times N_t}$

$N_t$: number of snapshots
$N_d$: degree-of-freedom of one snapshot ($N_x$*$N_y$)

(2) build the 2-point correlation matrix: $\boldsymbol{R} = \langle \boldsymbol{q}\boldsymbol{q}^{\mathrm{T}} \rangle = \frac{1}{N_t - 1}\boldsymbol{Q}\boldsymbol{Q}^{\mathrm{T}} = \frac{1}{N_t - 1}\sum_{i=1}^{N_t} \boldsymbol{q}_i \boldsymbol{q}_i^{\mathrm{T}}$

(3) solve the discrete EVP: $\boldsymbol{R}\boldsymbol{W}\boldsymbol{\Phi} = \boldsymbol{\Phi}\boldsymbol{\Lambda}$ (***W*** is the weight matrix consistent with the inner-product)

in practice, $N_t << N_d$, method of snapshot (Sirovich, 1987): $\frac{1}{N_t - 1}\boldsymbol{Q}^{\mathrm{T}}\boldsymbol{W}\boldsymbol{Q}\boldsymbol{\Psi} = \boldsymbol{\Psi}\boldsymbol{\Lambda}$

(4) recover the eigenmodes of ***q***: $\tilde{\boldsymbol{\Phi}} = \boldsymbol{Q}\boldsymbol{\Psi}\boldsymbol{\Lambda}^{-1/2}$

(5) complete the eigenvalue decomposition / singular value decomposition:

$$\begin{cases} \boldsymbol{R} = \tilde{\boldsymbol{\Phi}}\boldsymbol{\Lambda}\tilde{\boldsymbol{\Phi}}^{\mathrm{T}} \\ \boldsymbol{Q} = \tilde{\boldsymbol{\Phi}}\boldsymbol{\Sigma}\boldsymbol{\Psi}^{\mathrm{T}} \end{cases}$$

# 3. Data-driven coherent structure eduction

$$\boldsymbol{Q} = [\boldsymbol{q}_1, \boldsymbol{q}_2, \cdots, \boldsymbol{q}_{N_t}] \in \mathbb{R}^{N_d \times N_t}$$

$$\boldsymbol{Q} = \tilde{\boldsymbol{\Phi}}\boldsymbol{\Sigma}\boldsymbol{\Psi}^{\mathrm{T}}$$

The discrete POD expansion after numerical procedures:

$$\boldsymbol{q}(\boldsymbol{x}, t) = \sum_{i=1}^{N_t} a_i(t)\boldsymbol{\phi}_i(\boldsymbol{x}) \quad a_i(t) = \sqrt{\lambda_i}\psi_i(t)$$

- is a singular-value decomposition of the data matrix ***Q***

The energy optimality (note the eigenvalues have the dimension of energy): $\lambda_1 > \lambda_2 > \lambda_3 > \ldots > \lambda_N > 0$

$$E_N = \frac{1}{2}\sum_{n=1}^{N}\langle a_n^2(t)\rangle$$ - total energy, N = min($N_t$,$N_d$) = total rank

$$E_r = \frac{1}{2}\sum_{n=1}^{r}\langle a_n^2(t)\rangle$$ - truncated sum of the partial energy, r << N, low rank

For any truncation order r, the POD modes contain the largest truncated energy compared to any other orthogonal modes at the same order r, guaranteed by the optimality of singular value decomposition (SVD).

--> Applications of POD: flow structure extraction, Galerkin projected reduced-order dynamics, flow controls.

# 3. Data-driven coherent structure eduction

Example of POD: a cylinder wake flow (Noack et al., 2003 JFM)

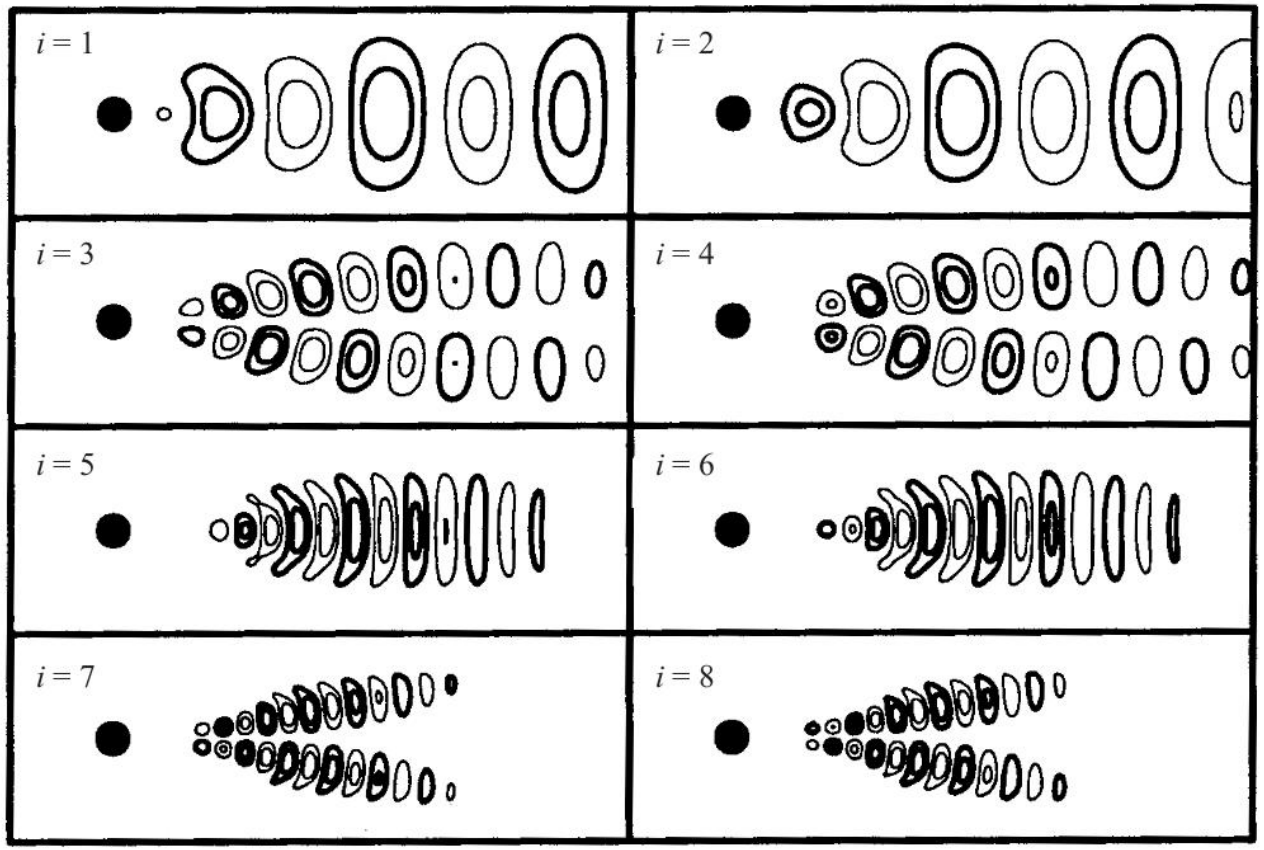


POD eigenmode shapes (modes 1-8)

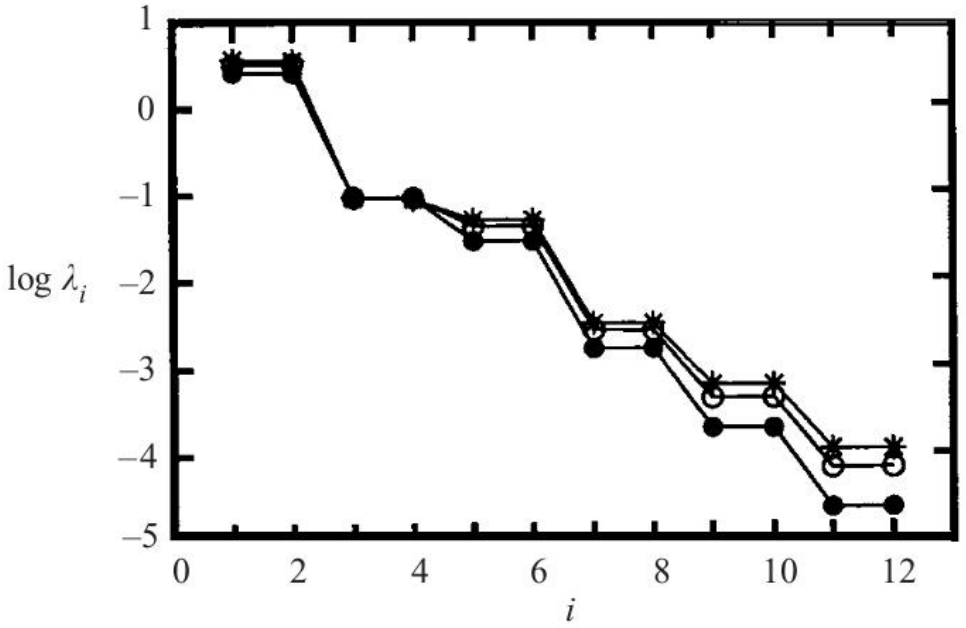


POD eigenvalues (modes 1-12)

- eigenvalues decay exponentially with mode index, suggesting that the flow can be well represented by a few (~10) modes.
- lower-rank modes (smaller *i*) typically represent larger structures

# 3. Data-driven coherent structure eduction

**Summary:** POD modes {phi$_n$(x)} are a set of orthogonal modes extracted from flow data / measurements. They are eigenfunctions of the two-point correlation tensor, each representing a fraction of the kinetic energy of the flow, ranked by the modal index (energy from high to low). POD modes in periodic directions degenerate to Fourier modes. POD is a substitute for Fourier expansion in the inhomogeneous directions.

$$u(\boldsymbol{x},t) = \sum_n a_n(t)\phi_n(\boldsymbol{x})$$

orthogonal eigenfunctions
('coherent structures')

expansion coefficients

Other names of POD: Karhunen–Loève decomposition (dynamical systems), principal component analysis (PCA, data analysis), empirical orthogonal function (EOF, oceanography) ...

Variants of POD: spectral POD (SPOD; Lumley 1970 book; Towne et al. 2018 JFM), balanced POD (Rowley 2005 IJBC)

Other modal decomposition methods: dynamic mode decomposition (DMD; Schmid 2010 JFM; Mezic 2013 ARFM), resolvent analysis (Jovanovic & Bamieh 2005 JFM; McKeon & Sharma 2010 JFM)

*Coherent structures, their origins, roles in turbulent flows, interactions with other structures and the background turbulence, modeling, control, are among those things that remain largely unknown, and what make turbulence still interesting.*